

# Damping rates of surface plasmons for particles of size from nano- to micrometers; reduction of the nonradiative decay

K. Kolwas\*\*, A. Derkachova\*

*Institute of Physics, Polish Academy of Sciences, Al. Lotników 32/46, Warszawa, Poland*

---

## Abstract

Damping rates of multipolar, localized surface plasmons (SP) of gold and silver nanospheres of radii up to  $1000\text{nm}$  were found with the tools of classical electrodynamics. The significant increase in damping rates followed by noteworthy decrease for larger particles takes place along with substantial red-shift of plasmon resonance frequencies as a function of particle size. We also introduced interface damping into our modeling, which substantially modifies the plasmon damping rates of smaller particles. We demonstrate unexpected reduction of the multipolar SP damping rates in certain size ranges. This effect can be explained by the suppression of the nonradiative decay channel as a result of the lost competition with the radiative channel. We show that experimental dipole damping rates [H. Baida, et al., *Nano Lett.* 9(10) (2009) 3463, and C. Sönnichsen, et al., *Phys. Rev. Lett.* 88 (2002) 077402], and the resulting resonance quality factors can be described in a consistent and straightforward way within our modeling extended to particle sizes still unavailable experimentally.

---

**Keywords:** plasmon damping, radiation damping, interface damping, surface plasmon resonance, multipolar plasmons, multipolar plasmon modes, Mie theory, gold nanoparticles, silver nanoparticles, nanosphere, nanoantenna, nanophotonics, plasmonics, size dependent optical properties, SERS, SP.

## 1. Introduction

The response of noble-metal nanoparticles to electromagnetic (EM) excitation is dominated by resonant excitations of localized surface plasmons (SPs) (see: [1, 2, 3, 4, 5] for reviews). When a metal particle is illuminated at corresponding resonance frequency, notably strong surface-confined optical fields can be generated. This property is applied in surface-enhanced Raman

---

\*Corresponding author

\*\*Principal corresponding author

*Email addresses:* [Krystyna.Kolwas@ifpan.edu.pl](mailto:Krystyna.Kolwas@ifpan.edu.pl) (K. Kolwas), [Anastasiya.Derkachova@ifpan.edu.pl](mailto:Anastasiya.Derkachova@ifpan.edu.pl) (A. Derkachova)

spectroscopy (SERS) [6, 7, 8], high-resolution microscopy [9] or improvement of plasmonic solar cells [10, 11, 12, 13, 14, 15]. Excitation of SPs at optical frequencies, non-diffraction-limited guiding of them (e.g. via a linear chain of gold nanospheres [8, 16, 17, 18, 19, 20]) and transferring them back into freely propagating light are processes of great importance in many applications. Gold and silver nanoparticles are important components for subwavelength integrated optics and high-sensitivity biosensors [4, 21, 22] due to their chemical inertness and unique optical properties in the visible to near-infrared spectral range.

Metal nanospheres are the simplest and the most fundamental structures for studying the basis of plasmon phenomena. Understanding the resonant interaction of light with plasmonic nanoparticles is also essential for applications, e.g. for designing useful photonic devices. The modeling of plasmon properties under the simplest electrostatic (quasistatic) approximation is valid only for particles much smaller than the wavelength of light; than size dependence of plasmon properties can be neglected. If a nanosphere is larger, the properties of the surface plasmons supported by this structure become dependent on the size of the particle [1, 23, 24, 25, 26, 27]. Size dependence of the retarded electronic response of a plasmonic particle is determined by the properties of metal at the SP resonance wavelength and the presence of the metal-dielectric interface.

Nanoparticles much smaller than optical wavelength first of all exhibit dipolar surface plasmon oscillations. Higher order multipolar resonances appear as new features in the optical spectra, at frequencies higher than that of the dipolar plasmon frequency. The spectral signatures of these higher order plasmon resonances were observed in elongated gold and silver nanoparticles [28, 29, 30] first. Fewer experimental investigations directly demonstrated the multipolar character of the observed resonances in spherical particles [26, 31, 32].

Controlling the spectral properties of a plasmonic nanosphere for technological or diagnostic applications is not possible without knowing the direct dependence of plasmon properties on particle size. Still it is believed (e.g. [5, 25]) that existing theories do not allow the rigorous direct calculation of the frequencies of the multipolar SP modes. However, apart from the plasmon resonance frequencies, also the plasmon decay rates (damping times) are essential in controlling the spectral response of the plasmonic particle. Total damping rates of multipolar SPs [27] define absorbing and emitting properties of a plasmonic nanoantennas which can be tuned by particle size. Nanoantenna of the right size can serve as an effective transitional structure which is able to absorb or to transmit electromagnetic radiation in plasmonic mechanism. The knowledge and modeling of plasmon damping effect as a function of particle size are thus of key interest for the development of plasmonic nanosystems. The central feature here is the actual enhancement of the electromagnetic field. It served as a stimulus for us for developing a strict and direct size characterization of multipolar plasmons resonance frequencies and plasmon damping rates.

Our extended modeling up to the radius  $R = 1000nm$ , and up to SP multipolarity  $l = 10$  allows us to determine the intrinsic properties of plasmonic spheres in the size range which has never been studied before. We do not apply any restrictions on the particle radius in relation to the wavelength of light; our study goes far beyond the particle size for which the quasistatic approximation is justified (e.g. [2, 5]).

The main reason of size sensitivity of SP which we discuss (usually referred to as the retardation effect ([33] and references therein)) is responsible for important red-shift of the plasmon resonance frequency for larger nanoparticles. It is accompanied by the significant increase in damping rate followed by noteworthy decrease for larger particles. In addition, we discuss the effect called the surface electron scattering effect [1] or interface damping [34] which causes the substantial modification of the plasmon damping rates in particles of sizes comparable or smaller than the mean electron free path. Sometimes called the "intrinsic size effect", it is described by the  $1/R$  dependence added to the electron relaxation rate  $\gamma$  of the dielectric function [1, 5, 35]. We perform both types of modeling including or neglecting the effect of surface scattering, in order to examine the causes of the size-dependent plasmon features.

Our extended modeling for large particles reveals new features of the total plasmon damping rate. We demonstrated, for the first time in spherical particles, the effect of reducing of multipolar SP damping rates below its low size limit which is equal to the nonradiative damping rate. Suppression of the total damping rates proven to exist in certain size ranges allowed a new insight into the role of radiation damping in the plasmon decay mechanism. We also describe changes of the quality Q-factor of SP multipolar resonances with particle size. Q-factor is used for determination of the local field enhancement [34] and effective susceptibility in nonlinear optical processes [36].

We also confront the size characteristics resulting from our modeling with the experimental results obtained for the dipole plasmon for gold [32, 34] and silver [37] particles of different sizes. We show that the measured dipole damping rates and quality factors [32, 34] can be described in a consistent and straightforward way within our modeling which deliver also predictions for particle of size range still unavailable experimentally.

## **2. Size dependence of SP parameters derived from optical spectra**

It is widely accepted, that excitation of surface plasmons (collective free-electron oscillations) is responsible for the commonly observed pronounced peaks in the optical absorption or extinction spectra. The spectra collected for nanoparticles of various sizes are used as a source of data allowing to reconstruct the change of the resonance (usually dipole only) position with size (e.g. [1, 34, 38]). The width of the peak is related to the (dipole) plasmon damping rate [32, 34, 37, 39, 40, 41].

Mie theory delivers an indispensable formalism enabling the description of scattering of a plane monochromatic wave by a homogeneous sphere of known radius, surrounded by a homogeneous medium [42, 43, 44, 45]. Mie formulas allow to predict the intensities of light scattered in a given direction or the absorption and scattering cross-section spectra for particles of a chosen size. The Mie spectra can be compared with the spectra (intensities of absorbed or scattered light) measured experimentally for particles of the same size.

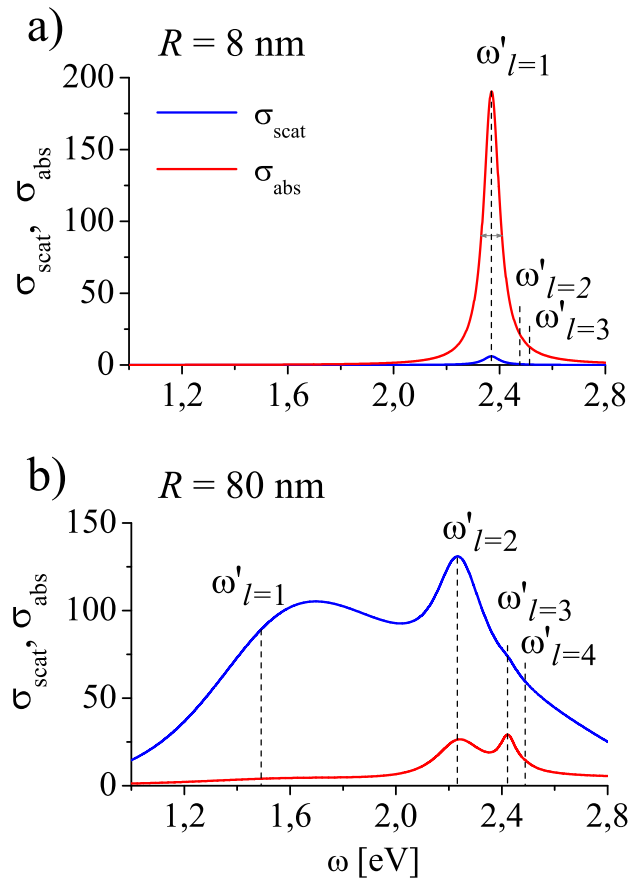


Figure 1: Absorption  $C_{\text{abs}}(\omega)$  and scattering  $C_{\text{scat}}(\omega)$  cross-sections for nanospheres of radii a) 8nm and b) 80nm (Mie theory). Figures illustrate suppression of absorption in larger particles. Broadening, deformation and shift of the maxima in the scattering spectra of larger particles in comparison with the SP resonance eigenfrequencies  $\omega'_l$  is also shown.

However, predicting the size dependence of multipolar plasmon resonance frequencies, Mie scattering theory is an inconvenient tool. SP size dependence can be determined only indirectly, by laborious derivation of positions of maxima in the consecutive spectra collected for various particle radii. The same applies to derivation of the size dependence of the (dipole) SP frequency

corresponding to the peak position from experimental data. In addition, the maximum in the spectrum ascribed to SP resonance can be broadened, deformed and shifted in respect to the frequency of plasmon oscillation mode [26, 27], as illustrated in Figure 1. That can affect the plasmon resonance position obtained from the experimental or calculated scattering spectra. It is even more difficult to determine the SP damping times from the width of the SP resonances, manifested in the optical spectra of larger particles, and to understand the derived size dependence then (e.g. [34, 37, 38]). The processes leading to plasmon damping are the subject of extensive research and debate (e.g. [1, 34, 39, 40, 46, 47, 48]). The homogeneous linewidth of the SP resonance was connected to the SP damping time. The properties of the SP are strongly influenced by this parameter. Mie scattering theory is not sufficient to define a general rule describing the size dependence of SP parameters; the damping rates and the resonance frequencies are not parameters of this theory.

### 3. Direct size characterization of multipolar SP modes

In order to derive parameters of SP as a function of particle size, we use an accurate electrodynamic approach based on [49], and described in more details in e.g. [50]. The formalism of Mie theory is used. However, the problem is formulated in absence of the illuminating light field; we are interested in intrinsic eigenproperties of the spherical particle (the analogy to the cavity eigenproblem) [26, 27]. In the present paper we extend the numerical calculations up to the radius of  $1000nm$  and plasmon polarity from  $l = 1$  up to  $l = 10$ . That allowed us to explore new features of localized SP excitations and reconsider the results of [27].

We consider continuity relations at the spherical metal/dielectric interface for the electromagnetic (EM) fields, which are the solutions of the Helmholtz equation in spherical coordinates  $(r, \theta, \phi)$  inside and outside the sphere. The transverse magnetic (TM) modes of EM waves localized on the interface possess a nonzero component of the electric field normal to the surface  $E_r$ , which can couple with free-electron charge oscillations at the boundary  $r = R$ . The conditions for the nontrivial solutions of the continuity relations for TM mode define the dispersion relation:

$$\sqrt{\varepsilon_{in}(\omega)}\xi_l'(k_{out}(\omega)R)\psi_l(k_{in}(\omega)R) - \sqrt{\varepsilon_{out}(\omega)}\xi_l(k_{out}(\omega)R)\psi_l'(k_{in}(\omega)R) = 0 \quad (1)$$

which is fulfilled for the complex eigenfrequencies of the field  $\Omega_l$  in successive multipolar modes  $l = 1, 2, 3, \dots$ .  $\psi_l(z)$  and  $\xi_l(z)$  are Riccati-Bessel spherical functions, the prime symbol ( $\prime$ ) indicates differentiation with respect to the argument,  $k_{in} = \frac{\omega}{c}\sqrt{\varepsilon_{in}(\omega)}$  and  $k_{out} = \frac{\omega}{c}\sqrt{\varepsilon_{out}}$ ,  $\varepsilon_{in}(\omega)$  and  $\varepsilon_{out}$  are the dielectric functions of a metal and of the particle dielectric surrounding, respectively. The dispersion relation (Equation(1)) is solved numerically for complex values of  $\Omega_l(R) = \omega_l'(R) + i\omega_l''(R)$  ( $\omega_l''(R) < 0$ ) for  $l$  in the range of  $1 \div 10$ . We solved the problem

for successive  $R$  values from 1 to 1000nm in 1nm steps. The *fsolve* function of the MatLab program, utilizing the *Trust-region dogleg* algorithm was used.

### 3.1. Material properties of plasmonic particles

The simplest analytic function often used to describe a wavelength dependence of optical properties of metals like gold or silver [51, 52, 53, 54, 55] results from the Drude-Lorentz-Sommerfeld model:

$$\varepsilon_D(\omega) = \varepsilon_0 - \omega_p^2/(\omega^2 + i\gamma\omega) \quad (2)$$

with  $\varepsilon_0 = 1$  (e.g. [1, 5]). The effective parameter  $\varepsilon_0 > 1$  describes contribution of bound electrons,  $\omega_p$  is the effective bulk plasma frequency which is associated with effective concentration of free-electrons,  $\gamma$  is the phenomenological damping constant of electron motion. For bulk metals  $\gamma = \gamma_{bulk}$  is related to the electrical resistivity of the metal and is supposed to include all microscopic damping processes due to photons, phonons, impurities and electron-electron interactions. In the present modeling we accept the following effective parameters of the dielectric function of the bulk gold:  $\varepsilon_0 = 9,84$ ,  $\omega_p = 9,010eV$ ,  $\gamma_{bulk} = 0,072eV$ .

The collision time  $1/\gamma_{bulk}$  determines the electron mean free path in bulk metals. At room temperatures the electron mean free path in gold is 42nm [1]. It can be comparable or larger than a dimension of a particle. An additional relaxation term added to the relaxation rate  $\gamma$  accounts for the effect of scattering of free electrons by the surface [1, 35, 41, 56, 57, 58]:

$$\gamma_R(R) = \gamma_{bulk} + A \frac{v_F}{R} \quad (3)$$

where  $v_F$  is the Fermi velocity ( $v_F = 1.4 \cdot 10^{-6}m/s$  in gold), and  $A$  is the theory dependent quantity of the order of 1 [1]. We accept the value  $A = 0.33$  in our modeling, according to [57]. Then the size-adopted bulk dielectric function is:

$$\varepsilon_{\gamma(R)}(\omega, R) = \varepsilon_0 - \omega_p^2/(\omega^2 + i\gamma_R(R)\omega) \quad (4)$$

The real part of  $\varepsilon_{\gamma(R)}$  is not modified by surface scattering. Frequency (and radius) dependence of the dielectric function (Equation 2 or 4) couples to the overall frequency (and radius) dependence of the plasmon dispersion relation (Equation(1)).

To underline the crucial role of interface damping in smaller particles, we will compare the results obtained with the dielectric function  $\varepsilon_{in} = \varepsilon_D(\omega)$  given by Equation (2) (with  $\gamma = \gamma_{bulk}$ , surface scattering neglected) and  $\varepsilon_{in} = \varepsilon_{\gamma(R)}(\omega, R)$  given by Equation (4) (with  $\gamma = \gamma_R(R)$ ). The dielectric function of the particle surrounding (vacuum/air) is assumed to be  $\varepsilon_{out} = 1$ , or is chosen to reflect the index of refraction of the particle environment, as described in Section 7, where we compare the results of our modeling with some experimental results of [34, 37].

### 3.2. Resonance frequencies and damping rates vs radius; the role of the interface damping

The solutions of the dispersion relation (Equation(1)) define the size dependence of multipolar plasmon oscillation frequencies  $\omega'_l(R) = Re(\Omega_l(R))$  and damping rates  $|\omega''_l(R)| = |Im(\Omega_l(R))|$  (and SP damping times  $T_l(R) = \hbar/|\omega''_l(R)|$ ) of the EM surface modes oscillations. We express  $\omega'_l, \omega''_l, \omega$  and  $\gamma$  in electronvolts (eV) for convenience.

The size dependence of  $\omega'_l(R)$  and  $|\omega''_l(R)|$  of SP modes for the first ten multipolar plasmons for gold spheres in vacuum/air ( $\epsilon_{out} = 1$ ,  $\gamma = \gamma_{bulk} = 0.072eV$ , the radius up to  $1000nm$ ) is presented in Figure 2. Black line ( $l = 1$ ) represents the dipole resonance frequency. Resonant excitation of SP oscillations takes place when the frequency of incoming light field  $\omega$  approaches the eigenfrequency of a plasmonic nanoantenna of a given radius  $R$ :  $\omega = \omega'_l(R)$ ,  $l = 1, 2, 3, \dots$ . If excited, plasmon oscillations are damped at corresponding rates  $|\omega''_l(R)|$  (Figure 2b)). Damping of surface plasmon oscillations is the inherent property of SP modes that defines absorbing and scattering properties of the plasmonic particle as a function of size.

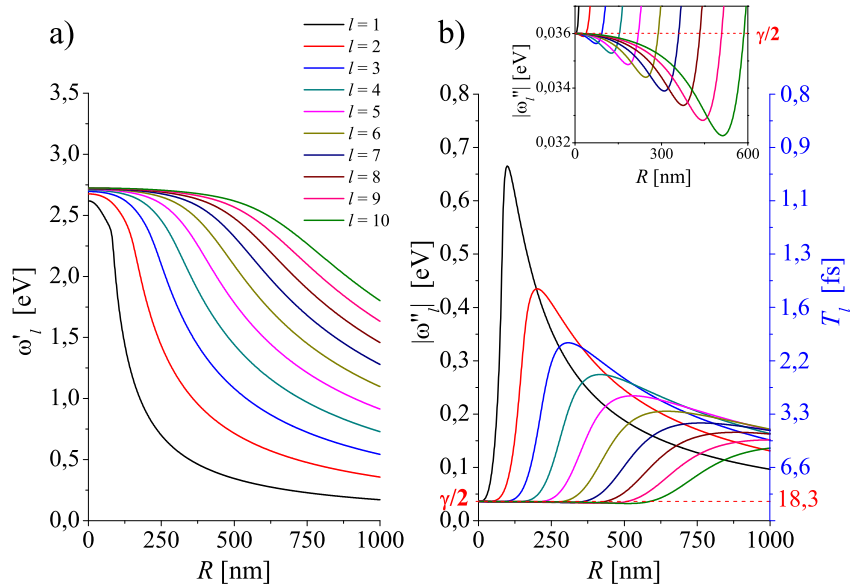


Figure 2: a) Multipolar plasmon resonance frequencies  $\omega'_l(R)$  and b) plasmon damping rates  $|\omega''_l(R)|$  (left axis) and corresponding damping times  $T_l$  (right axis) vs particle radius  $R$ . Reduction of the plasmon damping rates  $|\omega''_l(R)|$  below the nonradiative limit  $\gamma/2$  is demonstrated in the inset.

The SP frequencies  $\omega'_l(R)$  decrease with size monotonically, as illustrated in Figure 2a). For given particle radius  $R$ ,  $\omega'_l(R)$  increase with plasmon polarity  $l$ . The multipolar SP resonances for larger particles are better spectrally resolved than those for the smaller ones.

In the limit of small size, the analytic expressions for  $\omega'_l(R)$  and  $\omega''_l(R)$  can be found from the relation (1) after applying the power series expansion of the spherical Bessel and Hankel functions. Keeping only the first terms of the power series one can get:

$$\omega'_{0,l} = \left[ \frac{\omega_p^2}{\varepsilon_0 + \frac{l+1}{l}\varepsilon_{out}} - \left(\frac{\gamma}{2}\right)^2 \right]^{1/2}, \quad (5)$$

$$\omega''_{0,l} = -\frac{\gamma}{2}. \quad (6)$$

For a perfect free-electron metal ( $\varepsilon_0 = 1$ ,  $\gamma = 0$ ) and  $\varepsilon_{out} = 1$ , Equation (5) leads to the well-known plasmon frequencies within the "quasistatic approximation" [1, 50, 59]:  $\omega'_{0,l} = \omega_p/\sqrt{1 + \varepsilon_{out}(l+1)/l}$ , and in particular to the giant Mie resonance frequency  $\omega'_{0,l=1} = \omega_p/\sqrt{3}$  for  $l = 1$ .

In the smallest particles, the plasmon damping rates  $|\omega''_l(R)|$  fall to pure nonradiative damping rates  $|\omega''_{0,l}| = \gamma^{nr} = \gamma/2$ , as demonstrated in Figure 2b). The values of  $|\omega''_{0,l}|$  are the same for all multipolar plasmon modes  $l = 1, 2, 3\dots$  (Equation (6)). The nonradiative damping rates  $\gamma^{nr}$  are due to the ohmic losses if interface damping is neglected ( $\gamma = \gamma_{bulk}$ ), or are equal to  $\gamma_R/2$  (Equation 3) if interface damping is included in the modeling.

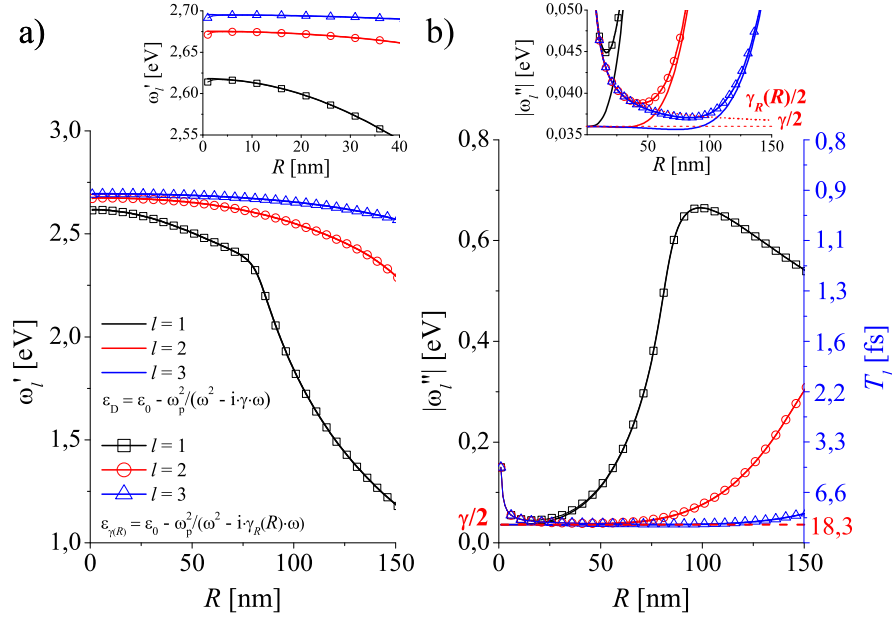


Figure 3: a) Dipole, quadrupole and hexapole plasmon resonance frequencies  $\omega'_l(R)$  and b) corresponding plasmon damping rates  $|\omega''_l(R)|$  calculated without (solid lines) and with (lines with hollow circles) interface damping taken into account. Insets are magnifications of figures a) and b) for particles of small radii.

Interface damping practically does not influence the size dependence of  $\omega'_l(R)$  as illustrated in Figure 3a). The minute red shift for the smallest sizes due to interface damping is shown in inset of Figure 3a). A similar finding results from the experimental observations [32, 34]. Therefore, the red shift of the (dipole) SP resonance frequency sometimes observed in small

particles versus decreasing size must result from some other phenomena due to the complex chemical effects and uncertainties in experimental samples [60].

In extended size range that we study, plasmon damping rates  $|\omega_l''(R)|$  are not simple monotonic functions of the radius (Figure 2b)). The initial fast increase of  $|\omega_l''(R)|$  with size is followed by gradual decrease for sufficiently large radii  $R$ . The increase in  $|\omega_{l+1}''(R)|$  in the subsequent  $l + 1$  SP modes is followed by the decrease in the SP damping rates  $|\omega_l''(R)|$  of lower polarity modes.

The surface scattering effect affects the total damping rate  $|\omega_l''(R)|$ , as illustrated in Figure 3b) and in the magnification of the part of this graph presented in Figure 4. The surface scattering contribution to the total relaxation rate  $\gamma_R(R)$  loses its importance for particles of radius larger than  $\sim 300nm$  (using the criterion  $(\gamma_R - \gamma)/\gamma_R \approx 1\%$ ).

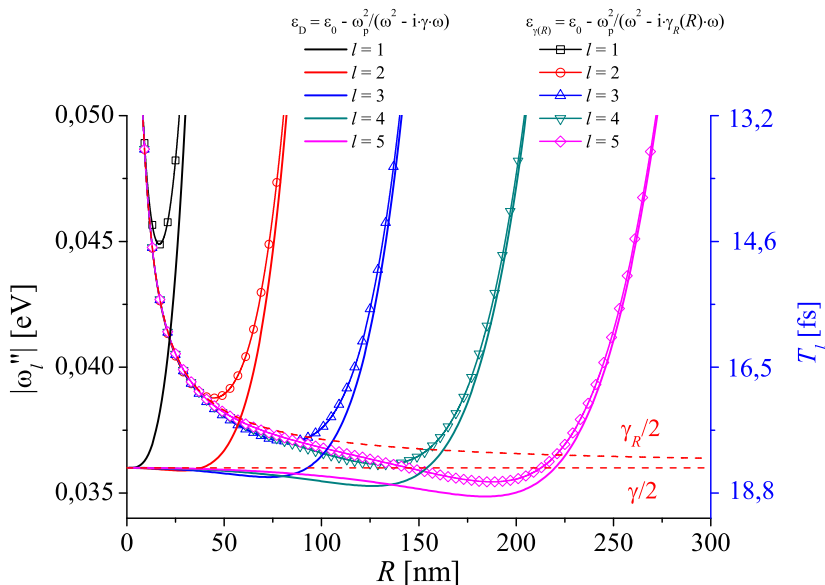


Figure 4: Demonstration of the reduction effect of plasmon damping rates  $|\omega_l''(R)|$  calculated without ( $\gamma = \gamma_{bulk}$ , solid lines) and with ( $\gamma = \gamma_R(R)$ , lines with hollow circles) interface damping; the magnification of a part of Figure 3.

#### 4. Radiative and nonradiative contributions to the total SP damping rates

The processes leading to damping of SP have been the subject of wide discussion and extensive studies, e.g. [1, 32, 34, 61, 62, 63] which, however, were limited to the dipole case. It was accepted that (dipole) SP in metal nanoparticles decays through both inelastic processes and elastic dephasing process which were usually neglected. Inelastic processes can be further divided into radiative and non-radiative decay processes [33, 34, 61]. The SP damping time  $T$  was determined from the homogeneous linewidth  $\Gamma = 2\hbar/T$  of a maximum in the spectrum

due to the SP dipole resonance. The observed spectral broadening of the maxima with size due to radiation is sometimes expected to be proportional to the particle volume [34, 57, 64]. Our results show (Figure 2b)), that the multipolar plasmon damping rates  $|\omega_l''(R)|$  are not simple, monotonic functions of particle radius. The initial fast increase of the total SP damping rate  $|\omega_l''(R)|$  with size is followed by gradual decrease for sufficiently large radii for the given mode  $l$ . Our modeling suggest that the proportionality of the multipolar radiation damping rate to  $R^3$  is not a general rule (see Figure 2b)).

Our extended modeling allows us to consider the higher order multipolar damping rates  $|\omega_l''(R)|$   $l=1,2\dots 10$ , as well. The total multipolar damping times  $\hbar/T_l$  can be related to the corresponding damping rates (homogeneous linewidths of the absorption [27] spectra  $\Gamma_l(R)$ ) and their size dependencies in a natural way:

$$\Gamma_l(R) = 2 |\omega_l''(R)| = 2\hbar/T_l \quad (7)$$

and

$$|\omega_l''| = \gamma_l^{rad} + \gamma^{nrad} \quad (8)$$

where  $\gamma^{nrad} = \gamma/2$ . The assumption, that the nonradiative and radiative processes (in dipole plasmon mode) are additive and are independent, is commonly accepted (see for example: [27, 41, 57, 58, 61]). However, expectation that the size dependence of the total damping rate  $|\omega_l''(R)|$  is due to the size dependence of the radiative damping rate  $\gamma_l^{rad}(R)$  only ( $|\omega_l''(R)| = \gamma_l^{rad}(R) + \gamma^{nrad}$ , [27]) must be reconsidered (see Section 5 below).

If the surface scattering effect is included,  $|\omega_l''(R)|$  becomes a decreasing function of size, starting from smaller particles (see Figure 3b) and 4, lines with symbols). The total SP damping rates follow the size dependence of nonradiative damping:  $\gamma_R(R)/2$ :  $|\omega_l''(R)| \approx \gamma_R(R)/2 = \gamma^{nrad}(R)$  in the range of radii which extends to larger  $R$  for growing SP polarity  $l$ . After reaching the minimum,  $|\omega_l''(R)|$  tends to follow the radius dependence unaffected by the interface damping.

A contribution of the radiation damping  $\gamma_l^{rad}(R)$  to the total damping rate  $|\omega_l''(R)|$  can be treated as a measure of the ability of the particle to couple to the incoming field and to emit light in plasmonic mechanism. As long as  $|\omega_l''(R)| \simeq \gamma^{nrad}$ , the SP mode  $l$  can only weakly couple with the incoming radiation and has weak radiative abilities. Consequently, the weakly radiative plasmons appear in the absorption spectra with a smaller amplitude and in scattering spectra (see Figure 1) they hardly manifest. With increasing  $l$ , SP plasmons gain the radiative character starting from larger particles due to the fact that  $\gamma_{l>1}^{rad}(R) > \gamma_{l-1}^{rad}(R)$ . Therefore, the higher order SP modes can be excited (and appear in the scattering spectra) for larger particles.

This fact is known from Mie scattering theory, but its physical sense have not been explained by Mie solutions.

## 5. Effect of reduction of multipolar plasmon damping rates

In the easier case (interface damping omitted in the modeling), reduction of the total SP dumping rates  $\gamma^{nrad}$  bellow the  $\gamma/2$  value (see the inset in Figure 2b)) manifests for plasmon modes with  $l > 1$ . This reduction effect can be clearly distinguished from other size dependent processes in some size ranges which grow with increasing  $l$ ; for the quadrupole ( $l = 2$ ) plasmon mode, the reduction effect extends up to  $R \simeq 40nm$ , for the hexapole ( $l = 3$ ) plasmon mode up to  $R \simeq 92nm$ , for  $l = 4$  up to  $R \simeq 155nm$  and so on.

We have checked, the reduction of the total damping rate is not present if  $\gamma = 0$  (2). On the contrary, it does not disappear if  $\gamma \neq 0$  and  $\varepsilon_0 = 1$ . That suggests, that if the additive form of the Expression (8) holds, reduction of the total plasmon damping rate is due to the decrease of nonradiative decay  $\gamma^{nrad}$  as compared with its low size limit  $\gamma^{nrad} = \gamma/2$  resulting from the energy dissipation of meatal (absorption). Consequently, the radiative and nonradiative contributions have to be coupled by their size dependence. The model with interface damping included, reproduces the SP rate reduction below  $\gamma^{nrad} = \gamma_R/2$  (see Figure 4), as well.

We can conclude, that reduction of  $|\omega_l''(R)|$  below the  $\gamma/2 = \gamma_{bulk}/2$  (or  $\gamma/2 = \gamma_R/2$ ) value takes place in the regions of sizes where the nonradiative damping is still not dominated by the fast radiative damping. Reduction in the total plasmon damping rate must be connected with suppression of the nonradiative decay channel. It can be inferred then, that the radiative and nonradiative processes are not independent. The effective rate of the nonradiative damping must be size dependent:  $\gamma^{nrad} = \gamma^{nrad}(R)$  with the value for the small particle limit:  $\gamma_0^{nrad} = \gamma/2$ . Suppression of the nonradiative damping is not restricted to the size ranges for which the effect was demonstrated, but influences the optical properties of plasmonic particles in a large range of sizes. Reduction of  $\gamma^{nrad}(R)$  manifests in the absorption spectrum of particles; absorptive abilities of large particles are poor as compared with small particles. This fact is described by solutions of Mie scattering theory, but its physical meaning have not been explained.

The effect of the total damping rate reduction with particle dimension was observed for the first time in the experiment with gold nanorods [34]. The size dependence of the dipole plasmon damping rate was deduced from the homogeneous linewidth  $\Gamma = 2\hbar/T$  of the maxima in the scattered intensities both for nanorods with various aspect ratios and spherical nanoparticles with radii in the range from 10 to 75nm. For nanorods, (dipole) plasmon damping rates decreased significantly for lower dipole plasmon oscillation frequencies. However, the decrease in the damping rate was not ascribed to the radiative processes. The authors of explain this

effect as reduction nonradiative plasmon decay by the fact that interband excitations in gold require a threshold energy of about  $1.8eV$  and expect, that suppression of the damping rate in such mechanism would also be present in gold spheres, but for plasmon resonance energies below  $1.8eV$ . Suppression of the plasmon damping rates in spheres had not been observed experimentally, as far as we know; the conclusive experimental data are limited to the plasmon dipole only, while according to our study the effect manifests for  $l > 1$ . Importance of the threshold energy at  $1,8eV$  in gold and exclusion of the radiative damping as a reducing mechanism was not confirmed by our study. On the contrary, the reduction of multipolar SP nonradiative damping rates results from competition between radiative damping  $\gamma_l^{rad}(R)$  and all other damping processes included in  $\gamma^{nrad}(R)$  and is present in plasmonic particles of any material.

## 6. Quality factor of multipolar plasmon resonances

Enhancement of optical response in resonance is usually described by the quality factor  $Q$ , defined as the product of the resonance center frequency and the bandwidth. In case of plasmonic particles the quality factor is interpreted as a measure of the local field enhancement [34] and is expected to define the effective susceptibility in nonlinear optical processes [36].

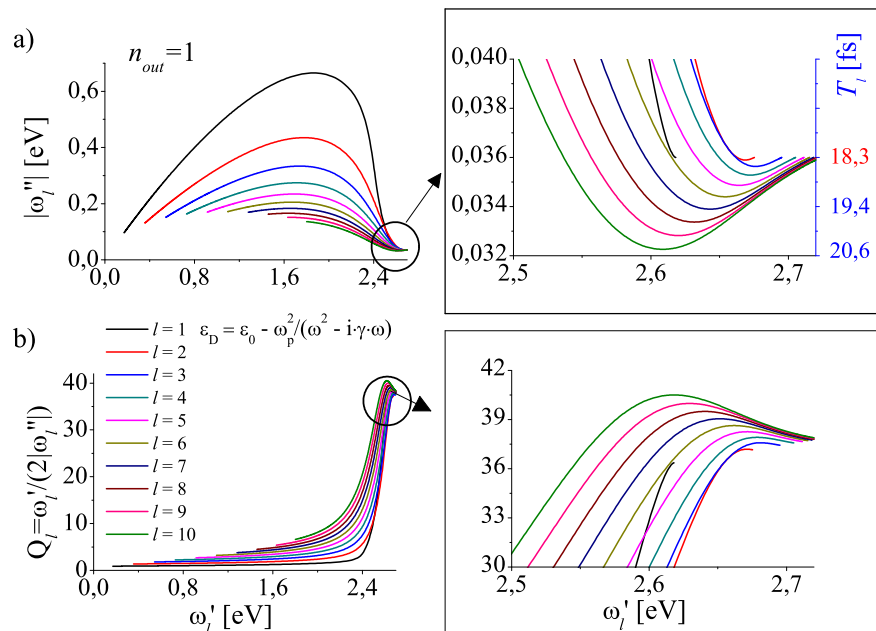


Figure 5: a) Damping rates  $|\omega_l''|$  vs  $\omega_l'$  for successive radii  $R$  and b) quality factors  $Q_l = \omega_l'(R)/(2|\omega_l''(R)|)$  for multipolar plasmon modes of gold nanoparticles ( $n_{out} = 1$ , surface scattering neglected). Graphs on the right are magnifications of circled regions of the graphs on the left.

The dependence of the  $\omega_l''$  vs  $\omega_l'$  for successive radii  $R$  and the resulting quality factors

$Q_l(R) = \omega'_l(R)/(2|\omega''_l(R)|)$  for multipolar plasmon modes of gold nanoparticles ( $n_{out} = 1$ ) are presented in Figures 5 (surface scattering neglected) and 6 (surface scattering included). The graphs on the right are the magnifications of the graphs (circled regions) on the left.

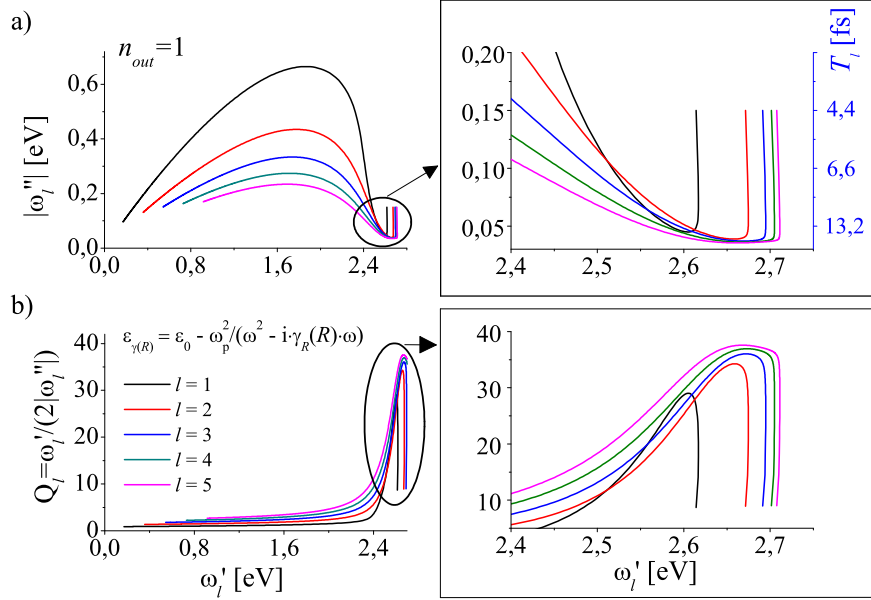


Figure 6: a) Damping rates  $|\omega''_l|$  vs  $\omega'_l$  for successive radii  $R$  and b) quality factors  $Q_l = \omega'_l(R)/(2|\omega''_l(R)|)$  for multipolar plasmon modes of gold nanoparticles ( $n_{out} = 1$ , surface scattering included). Graphs on the right are magnifications of circled regions of the graphs on the left.

Figure 5a) illustrates the effect of the total plasmon damping rate reduction to the value below  $\gamma^{nrad} = 0,032eV$  for modes with  $l > 1$ . Figure 5b) illustrates the resulting quality factors  $Q_l$  for successive SP modes which we use as a measure of energy stored in the SP oscillation of plasmon mode  $l$  at the resonance frequency  $\omega'_l(R)$ . In some ranges of SP resonance frequencies, the higher polarity plasmon modes ( $l > 1$ ) are more efficient in storing the SP oscillation energy. The similar conclusion comes from Figure 6b) (interface damping included). Quality factor of the dipole plasmon resonance reaches maximum value  $Q_{l=1} \approx 29$  for  $\omega'_l(R) \approx 2,606eV$  for gold nanoparticle of the radius  $R \approx 16nm$  (see Figure 7) and is the fast decreasing function of size for both smaller and larger particles. If a gold particle is embedded in a medium of higher optical density (see Figure 9,  $n_{out} = 1,5$ ), the maximum quality factor of the dipole plasmon resonance is even smaller,  $Q_{l=1} \approx 26$ . Such value corresponds to the resonance frequency of a gold particle of radius  $R \approx 11nm$ .

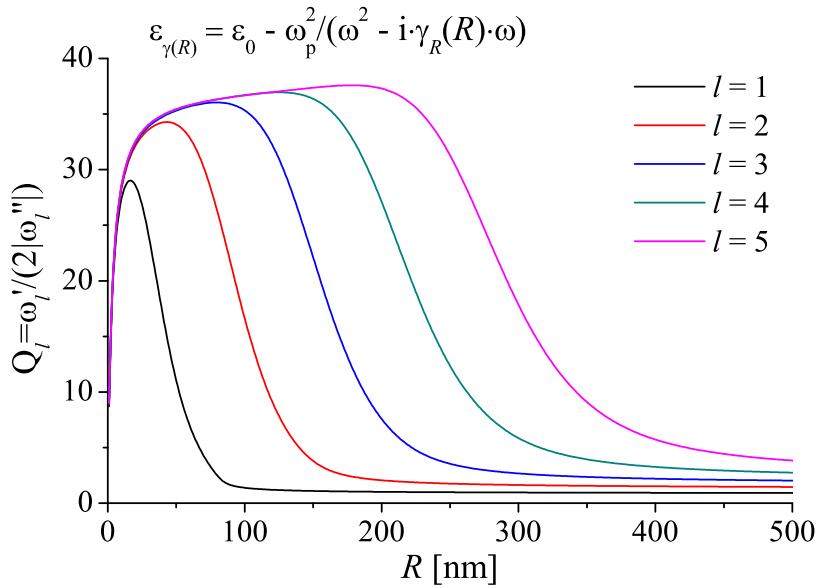


Figure 7: Quality factors  $Q_l$  vs radius  $R$  for multipolar plasmon modes of gold nanoparticles ( $n_{out} = 1$ , surface scattering included).

## 7. Dipole plasmon damping rates vs size: comparison with experimental results for silver and gold nanoparticles [34, 37]

Experimental investigations of spectral properties of plasmonic particles are usually performed on large particle ensembles, where inevitable variations in size, shape and surface properties tend to mask the spectral properties of the individual particles. The effects of surface chemistry (especially in Ag particles) and uncertainties in sample parameters affect linewidths and maxima positions which define damping times and resonance frequencies of SP. We have chosen two experiments [34, 37], which provide the spectroscopic data for individual spherical particles of silver and gold. The experiments were performed in well-controlled particle environments as a function of size for nanoparticles up to  $R = 25nm$  for silica-coated silver (Ag@SiO<sub>2</sub>) and for gold nanoparticles immersed in a index matching fluid ( $n_{out} = 1.5$ ) for relatively large range of radii (up to  $R = 75nm$ ). However, well resolved data was reported only for the dipole plasmon resonance. In Figures 8 and 9 we compare the experimental results presented in [34, 37] with the results of our modeling.

Figure 8 illustrates the spectral width  $\Gamma$  measured in different single Ag@SiO<sub>2</sub> nanoparticles vs the inverse of their equivalent diameter  $D_{eq}$ , optically determined by fitting the extinction spectra (see Figure 4 in [37]). Dashed line represents  $\gamma_R((2R)^{-1})$  dependence (Equation (3) for  $A = 0.7$  and  $\gamma_{bulk} = 0.125eV$ ). These parameters [37] result from a linear fit to the experimental data. Solid line results from our modeling in the extended range of sizes for  $\omega_p = 9.10eV$ ,

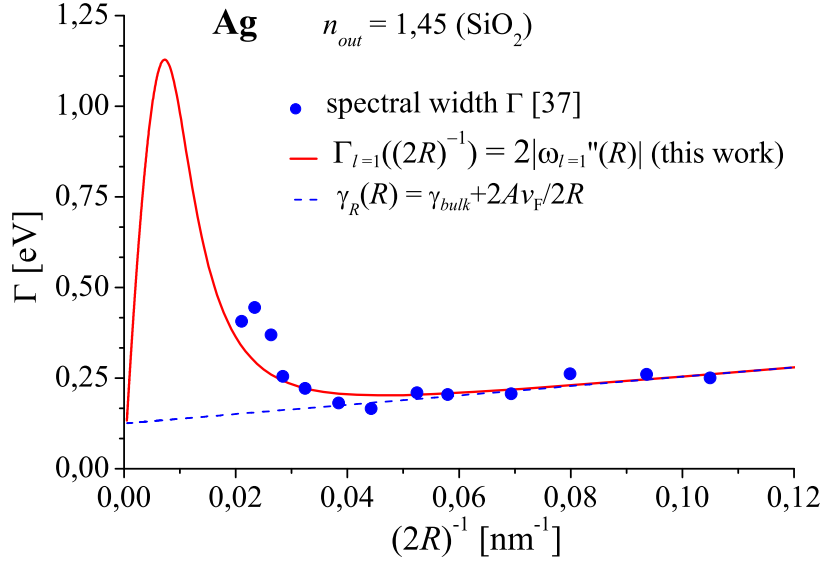


Figure 8: Spectral width  $\Gamma$  of plasmon resonances measured [37] in single spherical Ag@SiO<sub>2</sub> particles vs the inverse of their equivalent diameter. Dashed line represents  $\gamma_R((2R)^{-1})$  dependence (equation (3)), with the parameters  $A = 0.7$  and  $\gamma_{bulk} = 0.125eV$  resulting from linear fit to the experimental data [37]. Solid line results from our model with the parameters  $\omega_p = 9.10$ ,  $\varepsilon_0 = 4eV$ ,  $\gamma_{bulk} = 0.125eV$  and  $A = 0.7$ .

$\varepsilon_0 = 4eV$ ,  $\gamma_{bulk} = 0.125eV$  and  $A = 0.7$ . Our model with such input parameters reproduces the experimental data for smallest particles perfectly and describes the departure of  $\omega_{l=1}((2R)^{-1})$  dependence from linear. The  $\omega_l(R)$  model functions describe consistently the size dependence of the SP damping rates for experimentally available particles and predicts damping rates (and the resulting damping times) for larger sizes (experimentally unavailable so far) and for higher plasmon multipolarities.

Figure 9a) illustrates spectral widths  $\Gamma$  vs resonance energy  $\omega'_{l=1}(R)$  measured for different single Au nanoparticles (up to  $2R = 150nm$ ) (Figure 4 of [34]). The experimental data seems to suggest that  $\Gamma$  decays linearly with the SP resonance frequency. However, it is not the case. The dependence of  $\Gamma_{l=1}(\omega_{l=1}(R)) = 2|\omega''_{l=1}(R)|$  (line in figure 9a)) reproduces the experimental data and predicts the decrease in  $\Gamma_{l=1}$  for particles larger than those studied experimentally. Such decrease in damping rate  $|\omega''_{l=1}(R)|$  of the dipole SP is accompanied by the increase in the damping rate of the quadrupole  $|\omega''_{l=2}(R)|$  SP and of the following higher polarity SPs, as discussed in Section 5 (see Figure 2b)).

Figure 9b) illustrates the quality factor of the dipole resonance  $Q_{l=1} = \omega'_{l=1}(R)/2|\omega''_{l=1}(R)|$  vs resonance energy  $\omega'_{l=1}(R)$  (solid lines). Our modeling shows that interface damping (dashed line) substantially reduces the quality factor for particles from the smallest size range. The maximum factor  $Q_{l=1} \approx 26$  is found in nanoparticles of radii  $R = 12nm$ . The agreement with

the experimental data of [34] is very good.

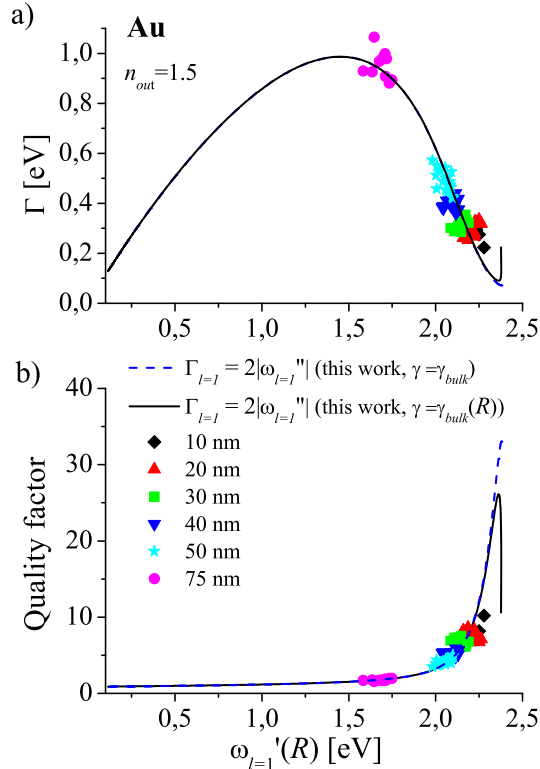


Figure 9: a) Spectral widths  $\Gamma$  of plasmon resonances vs resonance energy measured [34] in single spherical Au particles. b) Quality factor resulting from the experimental data. Lines represent the spectral width  $\Gamma_{l=1}(\omega_{l=1}(R)) = 2|\omega''_{l=1}(R)|$  and the quality factor  $Q_{l=1} = \omega'_{l=1}(R)/2|\omega''_{l=1}(R)|$  vs  $\omega'_{l=1}(R)$  for the dipole mode obtained from our modeling with surface damping neglected (dashed line) and included (solid line).

## 8. Conclusions

The dependence of the SP resonance frequencies  $\omega'_l(R)$  and damping rates  $|\omega''_l(R)|$  on particle radius determine the intrinsic optical properties of plasmonic spheres (illuminated or not). Our study provides direct, accurate size characteristics for a broad range of particle radii (up to  $R = 1000nm$ ) and plasmon polarities (up to  $l = 10$ ). At present, this exceeds the range experimentally explored.

Size dependence of SP damping rates  $|\omega''_l(R)|$  allows to distinguish the size ranges in which efficient transfer of radiation energy into heat takes place (large contribution of the nonradiative decay) and those in which the particles are effective radiating antennas (dominant contribution of the radiative damping). As long as the contribution of the radiative decay is negligible, the particle is not able to couple to the incoming field effectively and has weak radiative abilities. If the contribution of the radiative damping prevails, the particle is able to emit light within

plasmonic mechanism efficiently. Effective radiating enables efficient interaction of SP near-field with other structures at a desired resonance frequency  $\omega = \omega'_l(R)$ . The knowledge of size dependence of both: the multipolar SP resonance frequencies  $\omega'_l(R)$  and the corresponding damping rates  $|\omega''_l(R)| = \hbar/T_l(R)$  is indispensable to shape the particle plasmonic features effectively.

Our study, extended toward large particle sizes and plasmon multipolarities, revealed new features of the total plasmon damping rates. In certain ranges of radii, reduction of the multipolar SP damping rates, as compared with its small size limit, takes place. The small size limit is equal to the nonradiative damping rate resulting from absorption and heat dissipation. The suppression of nonradiative damping is not limited to the size range, in which the effect was directly demonstrated. It is present when the radiative damping brings the dominant contribution to the total plasmon damping. The reduction of  $\gamma^{nrad}(R)$  with the growing contribution of radiation damping is revealed in the absorption spectra of particles; absorptive abilities of large particles are poor. This fact is described by solutions of Mie scattering theory, but its physical background have not been explained, as far as we know. Our study led us to conclusion, that the reduction of multipolar SP nonradiative damping rates results from competition between radiative damping and all other damping processes included in  $\gamma^{nrad}(R)$ . As far as we know, such hypothesis has not been proposed before. Our study provides a new starting point for better understanding of rules that define contributions of plasmon radiative and nonradiative decay rates to the total SP decay rate as a function of particle size. The independent modeling is necessary for better understanding of the role of SP radiative and nonradiative decay channels.

The proposed SP characteristics vs particle size provide a consistent, uniform description of the experimental SP damping rates measured for single spherical particles in [34] and [37]. Not only dipole damping rates (found experimentally) but also multipole damping rates (and resulting damping times) in a broad range of sizes can be predicted.

The derived size dependence of plasmon decay rates  $|\omega''_l(R)|$  at resonance frequencies  $\omega'_l(R)$ , and the quality factors  $Q_l(R)$  of SP multipolar modes define not only the spectral scattering abilities of the plasmonic spheres, but also reflect changes in the strength of coupling of SP modes with the external field. Such characteristics can serve as a tool for controlling the spectral features of plasmonic nanospheres in technological or diagnostic applications, by optimizing the size at the desired resonance frequency  $\omega = \omega'_l(R)$ .

**Acknowledgement** We would like to acknowledge the financial support of this work by the Ministry of Science and Higher Education (No N N202 126837).

## References

- [1] U. Kreibig, M. Vollmer, *Optical Properties of Metal Clusters* (Springer Series in Material Science), Vol. 25, Berlin: Springer, 1995.
- [2] K. L. Kelly, E. Coronado, L. L. Zhao, G. C. Schatz, The optical properties of metal nanoparticles: the influence of size, shape, and dielectric environment, *J. Phys. Chem. B* 107 (2003) 668 – 677.
- [3] J. Z. Zhang, C. Noguez, Plasmonic optical properties and applications of metal nanostructures, *Plasmonics* 3 (2008) 127 – 150.
- [4] K. A. Willets, R. P. V. Duyne, Localized surface plasmon resonance spectroscopy and sensing, *Ann. Rev. of Phys. Chem.* 58 (2007) 267 – 297.
- [5] C. Noguez, Surface plasmons on metal nanoparticles: The influence of shape and physical environment, *J. Phys. Chem. C* 111 (2007) 3806 – 3819.
- [6] H. G. A Otto, I Mrozek, W. Akemann, Surface-enhanced raman scattering, *J. Phys.: Condens. Matter* 4 (1992) 1143 – 1212.
- [7] J. J. Mock, M. Barbic, D. R. Smith, D. A. Schultz, S. Schultz, Shape effects in plasmon resonance of individual colloidal silver nanoparticles, *J. Chem. Phys.* 116 (2002) 6755–6759.
- [8] S. A. Maier, H. A. Atwater, Plasmonics: Localization and guiding of electromagnetic energy in metal/dielectric structures, *J. Appl. Phys.* 98 (2005) 011101.
- [9] N. Fang, H. Lee, C. Sun, X. Zhang, Subdiffraction-limited optical imaging with a silver superlens, *Science* 308 (2005) 534 – 537.
- [10] B. P. Rand, P. Peumans, S. R. Forrest, Long-range absorption enhancement in organic tandem thin-film solar cells containing silver nanoclusters, *J. App.Phys.* 96 (2004) 7519 – 7526.
- [11] K. Catchpole, A. Polman, Plasmonic solar cells, *Optics Express* 16 (2008) 21793 – 21800.
- [12] S. Pillai, K. R. Catchpole, T. Trupke, M. A. Green, Surface plasmon enhanced silicon solar cells, *J. of Appl. Phys.* 101 (2007) 093105.
- [13] K. Nakayama, K. Tanabe, H. A. Atwater, Plasmonic nanoparticle enhanced light absorption in gaas solar cells, *App. Phys. Lett.* 93 (2008) 121904.

- [14] A. J. Morfa, K. L. Rowlen, T. H. R. III, M. J. Romero, J. van de Lagemaat, Plasmon-enhanced solar energy conversion in organic bulk heterojunction photovoltaics, *Appl. Phys. Lett.* 92 (2008) 013504.
- [15] S.-S. Kim, S.-I. Na, J. Jo, D.-Y. Kim, Y.-C. Nah, Plasmon enhanced performance of organic solar cells using electrodeposited ag nanoparticles, *Appl. Phys. Lett.* 93 (2008) 073307.
- [16] M. Quinten, A. Leitner, J. R. Krenn, F. R. Aussenegg, Electromagnetic energy transport via linear chains of silver nanoparticles, *Opt. Lett.* 23 (1998) 1331–1333.
- [17] S. A. Maier, M. L. Brongersma, P. G. Kik, H. A. Atwater, Observation of near-field coupling in metal nanoparticle chains using far-field polarization spectroscopy, *Phys. Rev. B* 65 (2002) 193408.
- [18] R. M. Dickson, L. A. Lyon, Unidirectional plasmon propagation in metallic nanowires, *J. Phys. Chem. B* 104 (2000) 6095 – 6098.
- [19] M. L. Brongersma, J. W. Hartman, H. A. Atwater, Electromagnetic energy transfer and switching in nanoparticle chain arrays below the diffraction limit, *Phys. Rev. B* 62 (2000) R16356 – R16359.
- [20] J. R. Krenn, A. Dereux, J. C. Weeber, E. Bourillot, Y. Lacroute, J. P. Goudonnet, G. Schider, W. Gotschy, A. Leitner, F. R. Aussenegg, C. Girard, Squeezing the optical near-field zone by plasmon coupling of metallic nanoparticles, *Phys. Rev. Lett.* 82 (12) (1999) 2590 – 2593.
- [21] B. Liedberg, I. Lundstrom, E. Stenberg, Principles of biosensing with an extended coupling matrix and surface plasmon resonance, *Sensors and Actuators B: Chemical* 11 (1993) 63 – 72.
- [22] K. Aslan, J. R. Lakowicz, C. D. Geddes, Plasmon light scattering in biology and medicine: new sensing approaches, visions and perspectives, *Current Opinion in Chemical Biology* 9 (2005) 538 – 544.
- [23] A. Derkachova, K. Kolwas, Size dependence of multipolar plasmon resonance frequencies and damping rates in simple metal spherical nanoparticles, *Eur. J. Phys. ST* 144 (2007) 93 – 99.
- [24] F. Tam, A. L. Chen, J. Kundu, H. Wang, N. J. Halas, Mesoscopic nanoshells: Geometry-dependent plasmon resonances beyond the quasistatic limit, *J. Chem. Phys.* 127 (2007) 204703.

- [25] S. Link, M. El-Sayed, Shape and size dependence of radiative, non-radiative and photothermal properties of gold nanocrystals, *International Reviews in Physical Chemistry* 19 (3) (2000) 409–453.
- [26] K. Kolwas, A. Derkachova, M. Shopa, Size characteristics of surface plasmons and their manifestation in scattering properties of metal particles, *J.Q.S.R.T.* 110 (2009) 1490 – 1501.
- [27] K. Kolwas, A. Derkachova, Plasmonic abilities of gold and silver spherical nanoantennas in terms of size dependent multipolar resonance frequencies and plasmon damping rates, *Opto-Electr. Rev.* 18 (2010) 429 – 437.
- [28] J. R. Krenn, G. Schider, W. Rechberger, B. Lamprecht, A. Leitner, F. R. Aussenegg, Design of multipolar plasmon excitations in silver nanoparticles, *Appl. Phys. Lett.* 77 (2000) 3379 – 3381.
- [29] K. L. Shuford, M. A. Ratner, G. C. Schatz, Multipolar excitation in triangular nanoprisms, *J. Chem. Phys.* 123 (2005) 114713.
- [30] E. K. Payne, K. L. Shuford, S. Park, G. C. Schatz, C. A. Mirkin, Multipole plasmon resonances in gold nanorods, *J. Phys. Chem. B* 110 (2006) 2150 – 2154.
- [31] K. Kolwas, S. Demianiuk, M. Kolwas, Dipole and quadrupole plasmon resonances in large sodium clusters observed in scattered light, *J. Chem. Phys.* 106 (1997) 8436 – 8441.
- [32] C. Sönnichsen, T. Franzl, T. Wilk, G. von Plessen, J. Feldmann, Plasmon resonances in large noble-metal clusters, *New J. Phys.* 4 (2002) 93.1–93.8.
- [33] R. Krahne, G. Morello, A. Figuerola, C. George, S. Deka, L. Manna, Physical properties of elongated inorganic nanoparticles, *Phys. Rep.* 501 (2011) 75 – 221.
- [34] C. Sönnichsen, T. Franzl, T. Wilk, G. von Plessen, J. Feldmann, O. Wilson, P. Mulvaney, Drastic reduction of plasmon damping in gold nanorods, *Phys. Rev. Lett.* 88 (2002) 077402.
- [35] S. Link, M. A. El-Sayed, Size and temperature dependence of the plasmon absorption of colloidal gold nanoparticles, *J. Phys. Chem. B* 103 (1999) 4212 – 4217.
- [36] V. Shalaev, E. Poliakov, V. Markel, Small-particle composites. ii. nonlinear optical properties, *Physical Review B* 53 (5) (1996) 2437.
- [37] H. Baida, P. Billaud, S. Marhaba, D. Christofilos, E. Cottancin, A. Crut, J. Lermé, P. Maioli, M. Pellarin, M. Broyer, et al., Quantitative determination of the size dependence of surface plasmon resonance damping in single  $\text{Ag}@SiO_2$  nanoparticles, *Nano Letters* 9 (10) (2009) 3463–3469.

- [38] P. K. Jain, X. Huang, I. H. El-Sayed, M. A. El-Sayed, Review of some interesting surface plasmon resonance-enhanced properties of noble metal nanoparticles and their applications to biosystems, *Plasmonics* 2 (2007) 107 – 118.
- [39] H. Hövel, S. Fritz, A. Hilger, U. Kreibig, M. Vollmer, Width of cluster plasmon resonances: Bulk dielectric functions and chemical interface damping, *Physical Review B* 48 (24) (1993) 18178.
- [40] S. Link, M. El-Sayed, Spectral properties and relaxation dynamics of surface plasmon electronic oscillations in gold and silver nanodots and nanorods, *The Journal of Physical Chemistry B* 103 (40) (1999) 8410–8426.
- [41] D. E. Charles, M. Gara, D. Aherne, D. M. Ledwith, J. M. Kelly, W. J. Blau, M. E. Brennan-Fournet, Scaling of surface plasmon resonances in triangular silver nanoplate sols for enhanced refractive index sensing, *Plasmonics* 6 (2011) 351 – 362.
- [42] M. Born, E. Wolf, *Principles of Optics*, Oxford: Pergamon, 1975.
- [43] C. F. Bohren, D. R. Huffmann, *Absorption and scattering of light by small particles*, New York: Wiley-Interscience, 1983.
- [44] J. A. Stratton, *Electromagnetic Theory*, International Series in Physics, McGRAW-HILL Book Company, Inc., 1941.
- [45] M. I. Mishchenko, L. D. Travis, A. A. Lacis, *Scattering, Absorption and Emission of Light by Small Particles*, Cambridge University Press: Cambridge, 2002.
- [46] T. Klar, M. Perner, S. Grosse, G. Von Plessen, W. Spirkl, J. Feldmann, Surface-plasmon resonances in single metallic nanoparticles, *Physical Review Letters* 80 (19) (1998) 4249–4252.
- [47] E. Heilweil, R. Hochstrasser, Nonlinear spectroscopy and picosecond transient grating study of colloidal gold, *The Journal of chemical physics* 82 (11) (1985) 4762.
- [48] Y. Liao, A. Unterreiner, Q. Chang, N. Scherer, Ultrafast dephasing of single nanoparticles studied by two-pulse second-order interferometry, *The Journal of Physical Chemistry B* 105 (11) (2001) 2135–2142.
- [49] R. Rupin, *Electromagnetic Surface Modes*, Wiley: Chichester, 1982.
- [50] R. Fuchs, P. Halevi, Basic Concepts and Formalism of Spatial Dispersion, in *Spatial Dispersion in Solids and Plasmas*, North-Holland, 1992.

- [51] P. G. Etchegoin, E. C. L. Ru, M. Meyer, An analytic model for the optical properties of gold, *J. Chem. Phys.* 125 (2006) 164705.
- [52] K.-S. Lee, M. A. El-Sayed, Gold and silver nanoparticles in sensing and imaging: sensitivity of plasmon response of size shape and metal composition, *J. Phys. Chem. B* 110 (2006) 19220 – 19225.
- [53] C. Oubre, P. Nordlander, Optical properties of metallodielectric nanostructures calculated using the finite difference time domain method, *J. Phys. Chem. B* 108 (2004) 17740 – 17747.
- [54] C. Noguez, C. E. Roman-Velazquez, Dispersive force between dissimilar materials: geometrical effects, *Phys. Rev. B* 70 (2004) 195412.
- [55] M. A. Ordal, R. J. Bell, R. W. Alexander, Jr, L. L. Long, M. R. Querry, Optical properties of fourteen metals in the infrared and far infrared: Al, co, cu, au, fe, pb, mo, ni, pd, pt, ag, ti, v, and w, *Appl. Opt.* 24 (1985) 4493 – 4499.
- [56] M. Quinten, Optical constants of gold and silver clusters in the spectral range between 1.5 eV and 4.5 eV, *Zeitschrift für Physik B Condensed Matter* 101 (2) (1996) 211–217.
- [57] C. Novo, D. Gomez, J. Perez-Juste, Z. Zhang, H. Petrova, M. Reismann, P. Mulvaney, G. V. Hartland, Contributions from radiation damping and surface scattering to the linewidth of the longitudinal plasmon band of gold nanorods: a single particle study, *Phys. Chem. Chem. Phys.* 8 (2006) 3540 – 3546.
- [58] M. Hu, C. Novo, A. Funston, H. Wang, H. Staleva, S. Zou, P. Mulvaney, Y. Xia, G. V. Hartland, Dark-field microscopy studies of single metal nanoparticles: understanding the factors that influence the linewidth of the localized surface plasmon resonance, *J. Mater. Chem.* 18 (2008) 1949 – 1960.
- [59] A. D. Boardman, B. V. Paranjape, The optical surface modes of metal spheres, *J. Phys. F: Metal Phys.* 7.
- [60] S. Peng, J. M. McMahon, G. C. Schatz, S. K. Gray, Y. Sun, Reversing the size-dependence of surface plasmon resonances, *PNAS* 107 (2010) 14530 – 14534.
- [61] E. J. Heilweil, R. M. Hochstrasser, Nonlinear spectroscopy and picosecond transient grating study of colloidal gold, *J. Chem. Phys.* 82 (1985) 4762 – 4770.
- [62] B. Lamprecht, J. Krenn, A. Leitner, F. Aussenegg, Particle-plasmon decay-time determination by measuring the optical near-fields autocorrelation: influence of inhomogeneous line broadening, *Appl. Phys. B* 69 (1999) 223 – 227.

- [63] F. Stietz, J. Bosbach, T. Wenzel, T. Vartanyan, A. Goldmann, F. Träger, Decay times of surface plasmon excitation in metal nanoparticles by persistent spectral hole burning, *Phys. Rev. Lett.* 84 (2000) 5644 – 5647.
- [64] A. Melikyan, H. Minassian, On surface plasmon damping in metallic nanoparticles, *Applied Physics B: Lasers and Optics* 78 (3) (2004) 453–455.